Kondo effect with Wilson fermions

Tsutomu Ishikawa,[1,2,3,*] Katsumasa Nakayama,[4,†] and Kei Suzuki[5,‡]

[1]*The Graduate University for Advanced Studies (SOKENDAI), Tsukuba 305-0801, Japan*
[2]*KEK Theory Center, Institute of Particle and Nuclear Studies, High Energy Accelerator Research Organization (KEK), Tsukuba 305-0801, Japan*
[3]*RIKEN Center for Computational Science, Kobe 650-0047, Japan*
[4]*NIC, DESY Zeuthen, Platanenallee 6, 15738 Zeuthen, Germany*
[5]*Advanced Science Research Center, Japan Atomic Energy Agency (JAEA), Tokai 319-1195, Japan*

(Received 16 July 2021; accepted 13 October 2021; published 29 November 2021)

We investigate the Kondo effect with Wilson fermions. This is based on a mean-field approach for the chiral Gross-Neveu model including four-point interactions between a light Wilson fermion and a heavy fermion. For massless Wilson fermions, we demonstrate the appearance of the Kondo effect. We point out that there is a coexistence phase with both the light-fermion scalar condensate and Kondo condensate, and the critical chemical potentials of the scalar condensate are shifted by the Kondo effect. For negative-mass Wilson fermions, we find that the Kondo effect is favored near the parameter region realizing the Aoki phase. Our findings will be useful for understanding the roles of heavy impurities in Dirac semimetals, topological insulators, and lattice simulations.

DOI: 10.1103/PhysRevD.104.094515

I. INTRODUCTION

The Kondo effect has a long history in solid-state physics [1–5]. It was observed as an enhancement of electric resistance of a metal, and it is induced by a strong correlation between nonrelativistic itinerant electrons and localized spin impurities. Kondo effects can be also realized for *relativistic* fermions such as Dirac/Weyl/Majorana fermions. Such relativistic Kondo effects can occur in relativistic-fermion systems including impurities, such as graphene (see Ref. [6] for a review), Dirac/Weyl semimetals [7–23], dense nuclear matter [24–27], and dense quark matter [13,24,28–44]. Among them, the "QCD Kondo effect" [24,28] is induced by the color exchange interaction between a light quark and an impurity quark, which is based on quantum chromodynamics (QCD). To determine the parameter region (or phase diagram) realizing the QCD Kondo effect is one of the challenging problems in QCD.

In this paper, we focus on the Kondo effect for the Wilson fermion. The Wilson fermion is one of the formulations realizing Dirac-like lattice fermions, which was first proposed in the viewpoint of construction of lattice gauge field theories [45,46]. It has been very useful to implement quark degrees of freedom in lattice QCD simulations, and also approximate Wilson fermions can be realized in Dirac semimetals.

In particular, the negative-mass region of the Wilson fermion is physically interesting because a part of this region corresponds to the bulk mode of topological insulators. In addition to the negative mass, an interaction between fermions, such as four-point or gauge interaction, can induce a new phase with spontaneous parity symmetry breaking for $N_f = 1$ (N_f is the number of flavors) or parity-flavor symmetry breaking for $N_f = 2$, which is the so-called Aoki phase [47]. The Aoki phase for the Wilson fermion was discussed by mean-field theories [47–54].[1,2] For QCD in continuum space, the Aoki phase is regarded as an artifact due to the discretization of the spacetime, but in solid-state physics, similar phase structures were pointed out by an interacting Su-Schrieffer-Heeger model [66], an interacting Kane-Mele model [67], and a Fu-Kane-Mele-Hubbard model [68]. Such parity-broken materials are also closely related to axion insulators (see Ref. [69] for a review). In this work, we investigate the interplay between the Aoki phase and the Kondo effect. Our studies will be useful for elucidating impurity effects in strongly correlated lattice fermion systems.

*tsuto@post.kek.jp
†katsumasa.nakayama@desy.de
‡k.suzuki.2010@th.phys.titech.ac.jp

[1]See Refs. [55–58] for arguments about an additional flavor-singlet condensate for $N_f = 2$.
[2]The Aoki phase can appear in other lattice-fermionic systems such as the domain-wall fermion [59–61], a naive or staggered fermion with a taste-splitting mass term [62], staggered-Wilson fermions [63], and minimal doubling fermions [64,65].

This paper is organized as follows. In Sec. II, we construct our model. In Sec. III, we show our numerical results and discuss properties of the Kondo effect with the Wilson fermion. Section IV is devoted to our conclusion and outlook.

II. FORMULATION

The Kondo effect for high-momentum particles can be described as a perturbative scattering problem between a light fermion and a heavy impurity. On the other hand, for the low-momentum region, the perturbative expansion does not converge, so that a nonperturbative approach is needed. In order to investigate the nonperturbative Kondo effect and its competition with other nonperturbative effects, we employ a mean-field approach. Mean-field approaches have been successfully applied to the conventional Kondo effect [70,71], and similar approaches should be also used for relativistic fermions (for a model with Nambu–Jona-Lasinio (NJL)-type four-point interactions, see Refs. [30,33]).

For the light-fermion sectors, we use the "chiral Gross-Neveu (χGN) model" in the $1+1$ dimensions [72] (namely, the NJL_2 model), which includes not only the scalar-type four-point interaction but also the pseudoscalar-type one. This model is used as a toy model for QCD. After replacing the (Dirac-type) continuous fermion by the Wilson fermion, we call this model the "Wilson-chiral-Gross-Neveu (WχGN) model." This model was first studied in Ref. [73], and, for early studies about the Aoki phase, see Refs. [47,48] at zero chemical potential and Ref. [52] at nonzero chemical potential.

For the sectors including heavy-fermion fields, we introduce a heavy-fermion field based on the heavy-quark effective theory (HQET) [74–77]. Although this field is regarded as a heavy-mass limit of the original massive Dirac field, it should be valid as long as its mass scale is sufficiently larger than its other typical scales. Furthermore, we use a four-point interaction between light and heavy fermions. Even if such a heavy-light four-point interaction may be regarded as an approximate form of the underlying interaction, it can be applied to nonperturbative physics such as strongly coupled heavy-light bound states (namely, mesons) [78–81] and the Kondo effect [30,33].

By combining the light- and heavy-fermion sectors, we can construct a "Wilson-chiral-Gross-Neveu-Kondo (WχGNK) model".[3] The Lagrangian in the $1+1$-dimensional continuous spacetime is given as

$$\mathcal{L} = \mathcal{L}_{\chi\mathrm{GN}} + \mathcal{L}_{\mathrm{K}}, \tag{1}$$

$$\mathcal{L}_{\chi\mathrm{GN}} = \bar{\psi}(i\partial\!\!\!/ - m_l)\psi + \mu\bar{\psi}\gamma^0\psi + \frac{G_{ll}}{2N}[(\bar{\psi}\psi)^2 + (\bar{\psi}i\gamma_5\psi)^2], \tag{2}$$

$$\mathcal{L}_{\mathrm{K}} = \bar{\Psi}_v iv^\mu\partial_\mu\Psi_v - \lambda(\bar{\Psi}_v\Psi_v - n_h) + \frac{G_{hl}}{N}[(\bar{\psi}\Psi_v)(\bar{\Psi}_v\psi) + (\bar{\psi}\gamma^1\Psi_v)(\bar{\Psi}_v\gamma^1\psi)], \tag{3}$$

where $\psi \equiv (\psi_1^T, \ldots, \psi_N^T)$ is a light Dirac fermion field with N components, and the bilinear operators are defined as, e.g., $\bar{\psi}\psi \equiv \sum_{k=1}^{N}\bar{\psi}_k\psi_k$. $N \geq 2$ can be regarded as the degeneracy factor from an $SU(N)$-symmetric interaction. m_l and μ are the mass and chemical potential of the light fermion, respectively. G_{ll} is the coupling constant between light fermions, which characterizes condensates composed of only light fermions.[4] G_{hl} is the coupling constant between a light fermion and a heavy fermion, which induces the Kondo effect (or the Kondo condensates). Note that a non-Abelian interaction between a light fermion and a heavy fermion is the necessary condition for the Kondo effect. For example, we can consider a Kondo effect with $N=2$ mediated by spin, isospin, pseudospin, or $SU(2)$-color exchange and $N=3$ by $SU(3)$-color exchange as in the usual QCD. The heavy-fermion field in the HQET is defined as $\Psi_v \equiv \frac{1+v^\mu\gamma_\mu}{2}e^{im_h vx}\Psi(x)$. In this form, the original N-component Dirac field $\Psi(x)$ at $x^\mu \equiv (t, x^1)$ in real space has a mass m_h. The heavy-fermion velocity v^μ is set as $v^\mu = (1,0)$, which is the so-called rest frame, and then the phase factor becomes $e^{im_h t}$. The original mass term is canceled by this phase factor in the kinetic term, so that it does not appear in the effective Lagrangian. $\Psi(x)$ is projected into its particle component by the particle projection operator $\frac{1+\gamma_0}{2}$. λ is the Lagrange multiplier for a constraint condition characterizing the heavy-fermion number density with N components defined as $n_h = \bar{\Psi}_v\Psi_v$, and we set $\lambda = 0$.

Next, using the Fourier transformation, we get the Lagrangian in momentum space. In order to get the Lagrangian on the lattice, we replace the spatial momentum p_1 in the kinetic term as follows:

$$p\!\!\!/ = \gamma_0 p_0 - \gamma_1 p_1 \to \gamma_0 p_0 - \frac{1}{a}\gamma_1 \sin ap_1 - \frac{r}{a}(1-\cos ap_1), \tag{4}$$

where a and r are the lattice spacing and the Wilson parameter, respectively. The fermion at $r=0$ is called the

[3] Precisely speaking, this model is analogous to the Coqblin-Schrieffer model [82] rather than the Kondo model [1], but we simply denote this model by "K."

[4] The χGN model at $m_l = 0$ satisfies the continuous chiral symmetry, but even at $m_l = 0$ the Wilson fermion breaks the chiral symmetry. If we are interested in the chiral symmetry in the continuum limit ($a \to 0$) of the WχGN model, two independent couplings for the scalar and pseudoscalar interactions are required [48]. The WχGNK model with two light-light couplings is also straightforward, but in this work we use the same coupling for simplicity.

naive fermion, and $r \neq 0$ is the Wilson fermion. In what follows, we set $r = 1$ and regard that the dimensional quantities are in the lattice unit ($a = 1$).

Note that, in our setup, the temporal direction related to p_0 is not on the lattice: the space is discretized, but the time is continuous. This situation corresponds to the usual lattice materials considered in solid-state physics. On the other hand, for a lattice simulation, the time is also discretized. In such a case, one can just replace p_0 by the similar form. Also, in the kinetic term of the heavy fermion, the spatial momentum is zero by taking the rest frame. Therefore, the heavy-fermion field depends on only p_0, so that we need not to replace p_1.

Here, we replace the four-point interactions by terms with three types of mean fields: the scalar condensate σ, pseudoscalar condensate Π, and Kondo condensates with a gap Δ. By analogy to the Kondo condensates for the Dirac fermion (the forms without M [30,33] or with M [34]), we assume the following forms:

$$\langle \bar{\psi}\psi \rangle \equiv -\frac{N}{G_{ll}}\sigma, \tag{5}$$

$$\langle \bar{\psi} i\gamma_5 \psi \rangle \equiv -\frac{N}{G_{ll}}\Pi, \tag{6}$$

$$\langle \bar{\psi}\Psi_v \rangle \equiv \frac{N}{G_{hl}}\Delta\sqrt{\frac{E_p + M}{E_p}}, \tag{7}$$

$$\langle \bar{\psi}\gamma^1\Psi_v \rangle \equiv \frac{N}{G_{hl}}\Delta\sqrt{\frac{E_p + M}{E_p}}\frac{-\sin p_1 + i\Pi}{E_p + M}, \tag{8}$$

where E_p and M are defined as

$$E_p \equiv \sqrt{\sin^2 p_1 + M^2 + \Pi^2}, \tag{9}$$

$$M \equiv 1 - \cos p_1 + m_l + \sigma. \tag{10}$$

The requirement of the two types (scalar and vector types) of Kondo condensates [30,33] reflects the particle-component projection for the light Dirac field. We keep the terms with the condensates, such as $\bar{\psi}\psi\langle\bar{\psi}\psi\rangle$, and neglect the second-order fluctuation terms. This procedure is equivalent to the large-N limit neglecting fluctuations of auxiliary boson fields.

The resulting mean-field Lagrangian is

$$\mathcal{L}_{\mathrm{MF}} = \bar{\phi}G^{-1}(p_0, p_1)\phi - \frac{N}{2G_{ll}}(\sigma^2 + \Pi^2) - \frac{2N}{G_{hl}}\Delta^2 + \lambda n_h, \tag{11}$$

where the inverse propagator of three-component quasiparticle $\phi \equiv (\psi^T, \Psi_v^T)$ in spinor space, composed of the two-component light fermion and the one-component heavy fermion, is

$$G^{-1}(p_0, p_1) = \begin{pmatrix} p_0 + \mu - M & \sin p_1 - i\Pi & \Delta^*\sqrt{\frac{E_p+M}{E_p}} \\ -\sin p_1 - i\Pi & -(p_0 + \mu) - M & -\Delta^*\sqrt{\frac{E_p+M}{E_p}}\frac{-\sin p_1 - i\Pi}{E_p+M} \\ \Delta\sqrt{\frac{E_p+M}{E_p}} & \Delta\sqrt{\frac{E_p+M}{E_p}}\frac{-\sin p_1 + i\Pi}{E_p+M} & p_0 - \lambda \end{pmatrix}. \tag{12}$$

Here, we used the gamma matrices: $\gamma^0 = \gamma_0 = \sigma_3$, $\gamma^1 = -\gamma_1 = i\sigma_2$, and $\gamma^5 = -\gamma_5 = \sigma_1$. By the diagonalization of the inverse propagator, we obtain the three dispersion relations of the quasiparticles,

$$E_\pm(p_1) \equiv \frac{1}{2}\left(E_p + \lambda - \mu \pm \sqrt{(E_p - \lambda - \mu)^2 + 8|\Delta|^2}\right), \tag{13}$$

$$\tilde{E}(p_1) \equiv -E_p - \mu, \tag{14}$$

where $E_\pm$ includes the effect of the Kondo condensate Δ, and $\tilde{E}$ is not affected by the Kondo condensate.

After summing up the Matsubara modes from the p_0 integral, the thermodynamic potential at inverse temperature $\beta = 1/T$ is written as

$$V(\sigma, \Pi, \Delta) = \frac{N}{2G_{ll}}(\sigma^2 + \Pi^2) + \frac{2N}{G_{hl}}\Delta^2 - \lambda n_h - N\int_{-\pi}^{\pi}\frac{dp_1}{2\pi}\left[\frac{1}{2}(\tilde{E} + E_+ + E_-) + \frac{1}{\beta}\ln[(1 + e^{-\beta\tilde{E}})(1 + e^{-\beta E_+})(1 + e^{-\beta E_-})]\right]. \tag{15}$$

By minimizing this potential as a function of (σ, Π, Δ), we can estimate the values of σ, Π, and Δ. Note that, in this form, since all the terms are proportional to N, the values of σ, Π, and Δ, as

plotted in the next section, do not depend on N. At zero temperature $\beta \to \infty$ and $\lambda = 0$, the effective potential is as follows:

$$V(\sigma, \Pi, \Delta; T \to 0, \lambda = 0) = \times \frac{N}{2G_{ll}}(\sigma^2 + \Pi^2) + \frac{2N}{G_{hl}}\Delta^2 - N\int_{-\pi}^{\pi}\frac{dp_1}{2\pi}(-\mu - \tilde{E} - E_-). \tag{16}$$

III. NUMERICAL RESULTS

A. Massless Wilson fermion

First we focus on the Kondo effect for the massless ($m_l = 0$) Wilson fermion. In Fig. 1, we show the μ dependence of σ and Δ at $G_{ll} = 1$. As shown in Fig. 1(a), when the heavy-light coupling G_{hl} is weak enough, the Kondo effect does not occur, where the phase diagram for σ is the same as that in the WχGN model (without the Kondo effect): we get $\sigma \approx 0.929$ at $\mu = 0$. From the figure, we find that there are two "critical" chemical potentials (or transition points), $\mu_{c1} \approx 0.91$ and $\mu_{c2} \approx 2.07$. μ_{c1} is the effect from the Fermi level, which is caused by a mechanism similar to the chiral symmetry restoration as in the χGN model. μ_{c2} is the effect from the lattice cutoff (or ultraviolet energy cutoff) for the Wilson fermion, as interpreted in terms of its dispersion relations (see later discussion).

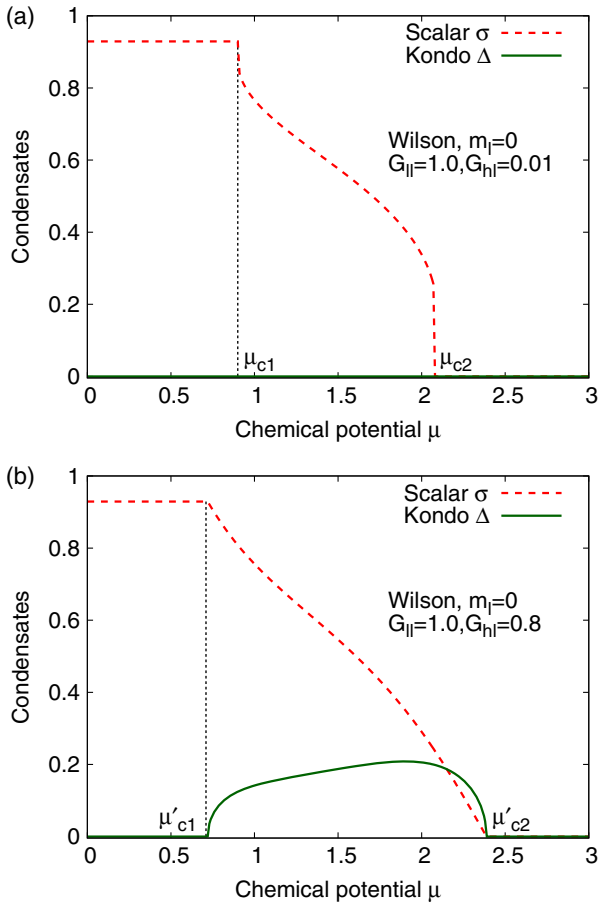

FIG. 1. μ dependences of σ and Δ for the massless Wilson fermion at (a) a weak heavy-light coupling $G_{hl} = 0.01$ and (b) a strong coupling $G_{hl} = 0.8$.

When the heavy-light coupling G_{hl} is strong enough, the Kondo effect occurs, as shown in Fig. 1(b). In the small-μ region at $G_{hl} = 0.8$, only the scalar condensate σ is realized. In the intermediate-μ region, the Kondo condensate Δ appears, and σ and Δ coexist. Here, as μ increases, σ is gradually reduced, and Δ increases. μ_{c1} for σ is shifted to lower $\mu'_{c1} \approx 0.72$ by the appearance of Δ. Thus, the transitions of both condensates occur at the same time. Intuitively, some of light fermions in this region start to form the Kondo condensate, and then they do not participate in the formation of the scalar condensate. As a result, μ_{c1} is shifted to lower μ'_{c1} by the appearance of the Kondo condensate. In the large-μ region with $\mu \gtrsim 2.39$, we find that both the condensates disappear. We also point out that μ_{c2} for σ is shifted to higher $\mu'_{c2} \approx 2.39$: the scalar condensate near μ_{c2} seems to be slightly enhanced by the Kondo effect. Thus, the shifts of critical chemical potentials, μ_{c1} and μ_{c2}, would be useful as evidence of the Kondo effect.

In order to interpret our results, in Fig. 2, we show the dispersion relations of the three particles at zero and nonzero μ at $G_{hl} = 0.8$ within the first Brillouin zone, where the explicit forms are given as Eqs. (13) and (14). The discussion from the dispersion relations is as follows:

(1) Small μ: If $\sigma = \Delta = 0$, as plotted as the black dashed and dotted curves in Fig. 2(a), then there is a band crossing point at $p_1 = 0$, which is the so-called Dirac point in the Wilson fermion. On the other hand, when

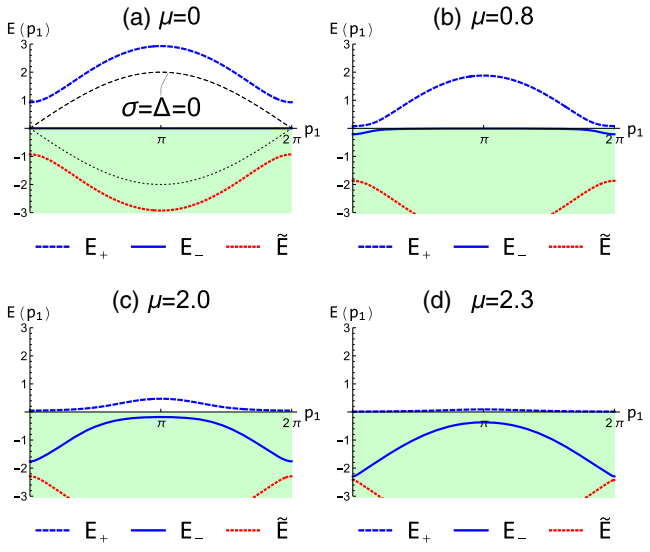

FIG. 2. Dispersion relations of particles at finite μ and $G_{hl} = 0.8$: E_+, E_-, and $\tilde{E}$. (a) $\mu = 0$, (b) $\mu = 0.8$, (c) $\mu = 2.0$, and (d) $\mu = 2.3$. The black dashed and dotted curves are the Wilson fermions at $\sigma = \Delta = 0$. The colored region means the Dirac or Fermi sea.

$\sigma \neq 0$ in the small-μ region, the scalar condensate opens a gap between the two dispersions, E_+ and $\tilde{E}$, as shown in Fig. 2(a). The dispersion relation $\tilde{E}$ of the negative-energy band is inside the Dirac sea (equivalently, the Fermi sea at $\mu = 0$) and stabilizes the system by the reduction of the free energy. Note that, in this region, E_- is equivalent to the flat band corresponding to the heavy fermion. Here, the Kondo effect is not realized (unless G_{hl} is large enough).

(2) Intermediate μ: If $\Delta = 0$, with increasing μ, the value of σ decreases. This is because the light-particle dispersion under the Fermi level is occupied, and $\sigma \neq 0$ leads to an enhancement of the free energy, compared to a dispersion with $\sigma = 0$. When the Kondo effect occurs ($\Delta \neq 0$), the light particle and the flat band are mixed by the Kondo condensate. As a result, E_- inside the Fermi sea stabilizes the system by the reduction of the free energy, as shown in Fig. 2(b) and 2(c).

(3) Large μ: In the large-μ region, the whole dispersion relation of the Wilson fermion is inside the Fermi sea, and the form of the dispersion is not affected by the condensates, as shown in Fig. 2(d). Note that when μ is large enough, E_+ closely resembles the flat band. Here, the Kondo effect is not realized, and the heavy fermion on the Fermi level and the massless Wilson fermion inside the Fermi sea are decoupled.

Next, we discuss the dependence on the coupling constant between the light fermions, G_{ll}. In Fig. 3, we show the phase structure on the μ-G_{ll} plane at $G_{hl} = 0.8$, where the gray region represents the plane at $\sigma = \Delta = 0$. When G_{ll} is small enough, there is the coexistence phase of the scalar and Kondo condensates. In the region at large G_{ll} and small μ, the Kondo effect is excluded, and then a pure scalar-condensate phase is realized. On the other hand, the region at large G_{ll} and large μ becomes the coexistence phase (within the plotted region). Note that, in the large-chemical-potential region with $\mu \gtrsim 2.39$, neither of the two condensates can be realized because of the lattice cutoff effect as shown in Fig. 2(d). Such a second critical chemical potential does not depend on G_{ll}.

In the Appendix, we show the results for Kondo effects with the Dirac fermion and naive lattice fermions.

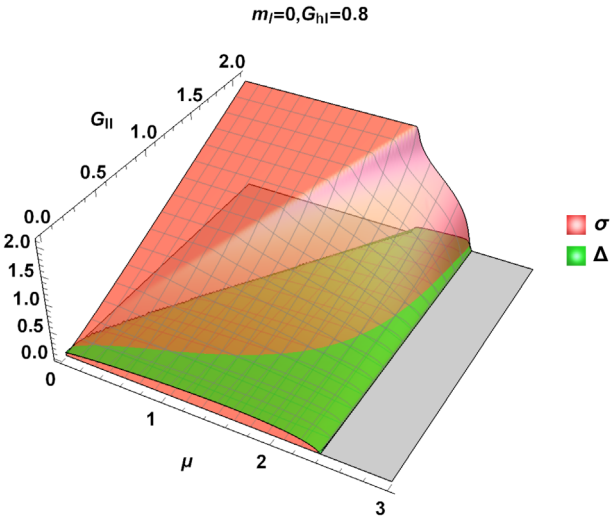

FIG. 3. Phase structure of σ and Δ on the μ-G_{ll} plane at $m_l = 0$ and $G_{hl} = 0.8$.

B. Negative-mass Wilson fermion

Here, we investigate the interplay between the Aoki phase and the Kondo effect. In the region with a positive mass $m_l > 0$ for the Wilson fermion, the Aoki phase does not appear ($\Pi = 0$). When a negative mass $m_l < 0$ is switched on, the Aoki phase ($\Pi \neq 0$) can be realized in a parameter region.

In Fig. 4, we show the negative-mass dependence of the condensates, where we fixed $G_{ll} = 1.5$ to focus on the Aoki phase with a sufficiently large value of the pseudoscalar condensate. Also, in this figure, we fix $\mu = 0$ and change only G_{hl} as a parameter tuning the Kondo effect. As in Fig. 4(a), when the heavy-light coupling is weak

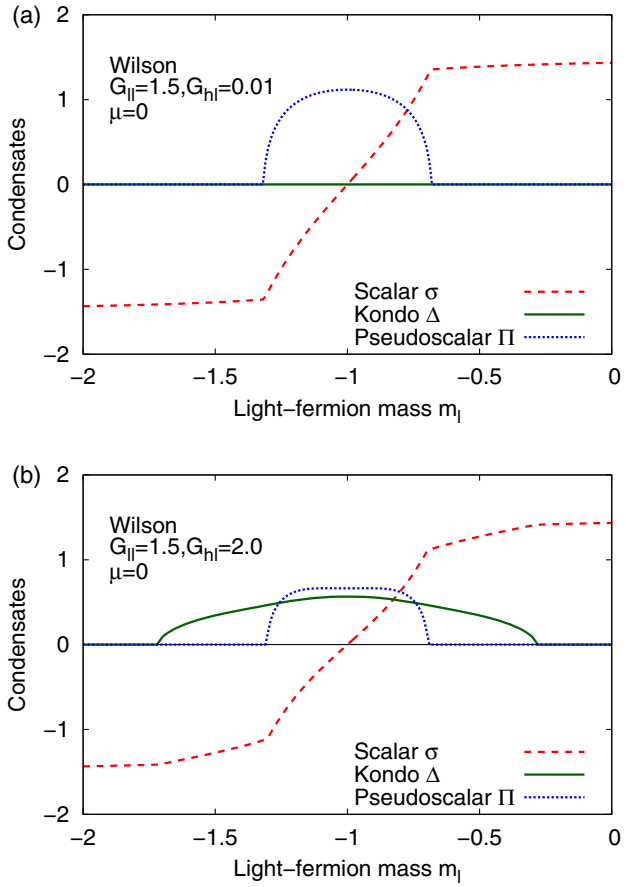

FIG. 4. m_l dependences of condensates for the negative-mass Wilson fermion at (a) a weak heavy-light coupling $G_{hl} = 0.01$ and (b) a strong coupling $G_{hl} = 2.0$.

enough ($G_{hl} = 0.01$), the Kondo effect does not occur, and only the scalar and pseudoscalar condensates are realized. These behaviors are well known as the conventional Aoki phase scenario in the WχGN model.

In Fig. 4(b) we show the results at $G_{hl} = 2.0$. Here, the heavy-light coupling is large enough, so that the Kondo effect is realized and modifies the other condensates. From this figure, our findings are as follows:

(1) We find nonzero values of the Kondo condensate around $m_l = -1$, and it coexists with the Aoki phase. In particular, the Kondo effect is most favored at $m_l = -1$. This behavior is similar to the Aoki phase in the strong-coupling region.

(2) We find that the Kondo effect suppresses both the absolute values of the scalar and pseudoscalar condensates. Intuitively, this is because light fermions form the Kondo condensate, and then they do not participate in the scalar or pseudoscalar condensate. Therefore, in experiments or lattice simulations, if one observes such a suppression of the scalar or pseudoscalar condensate, it will be evidence of the Kondo effect.

In Fig. 5, we show the phase structure of σ, Π, and Δ on the $m_l - G_{ll}$ plane at $\mu = 0$ and $G_{hl} = 0.8$ or 2.0. Note that, to improve the visibility, we plot $\sigma + m_l$ instead of σ. From this figure, we find that Δ is favored in the weak G_{ll} region. In particular, at $G_{hl} = 0.8$, the Kondo condensate appears only in the parameter regions that should have been the Aoki phase at $G_{hl} = 0$ (the so-called Aoki fingers or cusp region). This is because the dispersion relation at $m_l = 0$ or $m_l = -2$ is gapless at $p_1 = 0$ or $p_1 = \pi$, and such a gapless band is closer to the flat band of the heavy fermion. On the other hand, the dispersion relation at $0 < m_l < -2$ is gapped at any momentum, which is away from the heavy-fermion band. In the region with the Kondo condensate, the value of the pseudoscalar condensate is suppressed, and the original Aoki phase can be excluded by the Kondo effect. In other words, the Aoki fingers are covered by "fingernails" of the Kondo condensate phase. Furthermore, at stronger heavy-light coupling ($G_{hl} = 2.0$), we find a wide region of the Kondo condensate, which expands to larger-G_{ll} region. Thus, our results indicate that the effects from heavy impurities (via G_{hl}) can be significant in weakly coupling region for G_{ll}.

In order to discuss the μ dependence, in Fig. 6, we show the phase structure on the μ-G_{ll} plane at $G_{hl} = 0.8$ and $m_l = -1.1$.[5] As μ increases, the pseudoscalar condensate decreases, while the Kondo condensate increases. Around the transition point of μ, the scalar condensate is also modified. Similar to Fig. 3 at $m_l = 0$, when the chemical potential is large enough, all condensates are zero by the lattice cutoff effect.

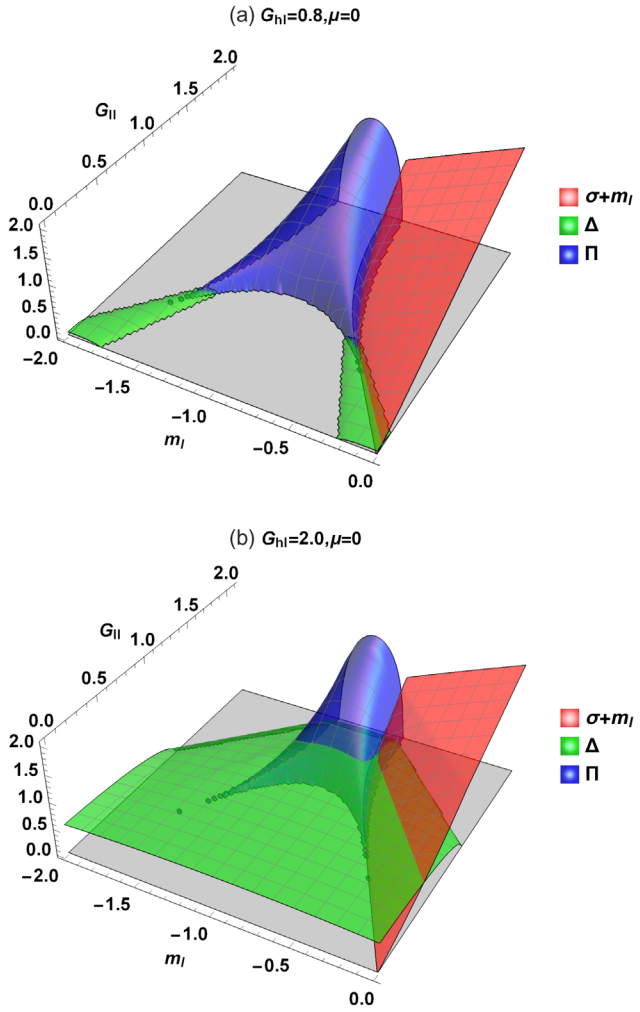

FIG. 5. Phase structure of σ, Δ, and Π on the m_l-G_{ll} plane at $\mu = 0$ and (a) $G_{hl} = 0.8$ or (b) $G_{hl} = 2.0$.

We emphasize that the negative-mass region of the Wilson fermion can be regarded as an effective model for the bulk of topological insulators.[6] The two parameters in the Hamiltonian of the Wilson fermion, the mass $m_l < 0$ and the Wilson parameter r, can be related to the band structure of a material, which is determined by the original band and the strength of the spin-orbit interaction. An intrinsic spin-orbit interaction may be roughly tuned by changing the chemical composition of the material (e.g., for $BiTl(S_{1-\delta}Se_{\delta})_2$, see Ref. [85]). In this sense, one can experimentally examine the negative-mass dependence. As in Fig. 5(a), we have found that the phase transitions (namely, appearance or disappearance) of the Kondo condensate Δ significantly depend on the negative mass m_l.

[5]Note that $m_l = -1$ is a special parameter because the dispersion relations become two flat bands (for light fermions). Such a situation is interesting as physics of the flat band (e.g., see Refs. [83,84]), but we focus on the Wilson fermion at $m_l = -1.1$ in the main text.

[6]In particular, the weak-coupling region in $1 + 1$ dimensions for odd N is a topological insulator belonging to the symmetry class BDI [53], where a topological invariant is characterized by the Zak phase defined as the integral of the Berry connection.

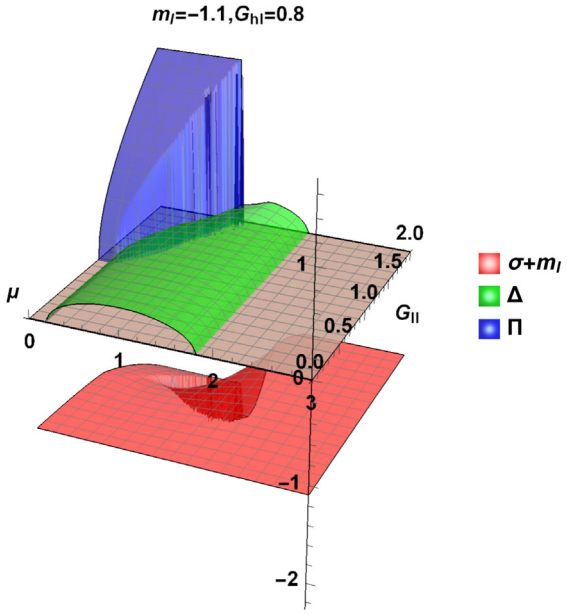

FIG. 6. Phase structure of σ, Δ, and Π on the μ-G_{ll} plane at $m_l = -1.1$ and $G_{hl} = 0.8$.

Therefore, experimentally, one could capture such a phase transition by tuning the spin-orbit interaction.

On the other hand, for topological insulators, the coupling constant (corresponding to G_{ll}) between electrons is usually small, so that the parameter region with the Aoki phase may be narrow. Instead of topological insulators in the strong-coupling region, the axion insulators (see, e.g., Ref. [69]) are other candidates to study the interplay between a parity-symmetry breaking ground state and the Kondo effect. In order to build an effective model to describe axion insulators, we have to introduce a pseudoscalar-mass term such as $im_5\bar{\psi}\gamma_5\psi$. Investigation of Kondo effects based on such an effective model will be straightforward. From our results shown in this paper, we can expect impurity effects in axion insulators by regarding the pseudoscalar condensate Π as the pseudoscalar mass m_5. For example, we can expect the appearance of the Kondo effect at a small m_5 and the suppression of the Kondo effect by a large m_5.

IV. CONCLUSION AND OUTLOOK

In this paper, we have investigated the Kondo effect for the Wilson fermion with the four-point interaction, which is based on the discretization (4) of the χGNK model (1). From our model, we have found (i) a coexistence phase of the Kondo condensate and other condensates such as the scalar and pseudoscalar condensates, (ii) a shift of the critical chemical potential of the scalar condensate by the Kondo effect, and (iii) an interplay between the Kondo effect and Aoki phase (particularly, the Kondo fingernails structure).

It should be noted that our WχGNK model is a choice of models describing the Kondo effect for the Wilson fermion, and other types of WχGNK models may be also constructed. For example, we have used the heavy-fermion field based on the *leading order* of HQET, but the building of WχGNK models based on its higher orders or heavy Dirac fermions will be also interesting. Furthermore, the mean-field assumptions might be improved. We have assumed the condensates (5)–(8), but other types of light-fermion condensates and Kondo condensates, e.g., including spatially inhomogeneous condensates, might be possible. Such a detailed examination is left for future studies. Also, it will be interesting to extend our model to higher spatial dimensions, such as the NJL_3 and NJL_4 models, or to replace the four-point interactions by other interactions, such as non-Abelian gauge interactions.

In this work, we have focused only on the situations with a single light flavor (the number of flavors is not N but N_f), which will be examined by $N_f = 1$ lattice simulations. We comment on the extension to the $N_f = 2$ case. In this case, additional flavor degrees of freedom may lead to "overscreening" of the Kondo effect, and non-Fermi-liquid behavior can appear, which is the so-called multichannel Kondo effect [86] (see Refs. [13,32] for expectations for the QCD Kondo effect). In such a situation, the standard mean-field approximation may be useless, and then one has to use an alternative approach, such as $N_f = 2$ lattice simulations. As a direct measurement for the Kondo effect in lattice simulations, one may measure the vacuum expectation value of a heavy-light bilinear operator, such as $\langle\bar{\psi}\Psi_v\rangle$ defined in this paper. Also, the values of light-fermion condensates $\langle\bar{\psi}\psi\rangle$ and $\langle\bar{\psi}i\gamma_5\psi\rangle$ are modified by the Kondo effect, and they will be indirect evidence of the Kondo effect. Furthermore, heavy-light mesonic two-point correlators also could be influenced by the Kondo effect.

Monte Carlo simulations of the WχGN model at finite chemical potential may suffer from the sign problem. In this case, one can expect the realization of the Kondo effect by tuning the heavy-light coupling constant. Also, even at finite chemical potential, sign-problem-free approaches, such as the tensor renormalization group [87], the matrix product state [53], and the projected-entangled-pair state [54], will be useful.

In addition, cold-atom simulations may be also promising candidates for examining both the interacting Wilson fermion [88–91] and the Kondo effect, e.g., [92–100], where tuning the coupling constants rather than the chemical potential will be useful for elucidating the Kondo effect.

ACKNOWLEDGMENTS

The authors thank Yasufumi Araki, Daiki Suenaga, and Shigehiro Yasui for helpful discussions. This work was supported by Japan Society for the Promotion of Science (JSPS) KAKENHI (Grants No. JP17K14277 and No. JP20K14476). T. I. was supported by RIKEN Junior Research Associate Program.

APPENDIX: KONDO EFFECTS FOR DIRAC AND NAIVE FERMIONS

In this Appendix, we qualitatively compare Kondo effects for other fermions with that for the Wilson fermion. Here we focus on the Dirac fermion and naive lattice fermion in $1+1$ dimensions: we investigate the phase structures of the "Dirac-chiral-Gross-Neveu-Kondo model," defined as the Lagrangian (1), and the "naive-chiral-Gross-Neveu-Kondo model," defined using the discretization (4) at $r=0$.

In Fig. 7, we show the results for the Dirac fermion, where the momentum integral interval in the effective potential is $-\Lambda \le p_1 \le \Lambda$ with a cutoff Λ.[7] In the intermediate-μ region, the coexistence phase of σ and Δ appears, which is similar to that of the Wilson fermion. In the large-μ region, σ becomes zero, whereas Δ survives. Such behavior is distinct from the case of the Wilson fermion in which σ and Δ becomes zero at the same time because of the lattice cutoff.

In Fig. 8, we also show the results for the naive fermion. The behavior in the intermediate-μ region is similar to the Wilson and Dirac fermions. In the large-μ region, σ becomes zero. At higher μ, Δ also becomes zero by the lattice cutoff effect. Thus, the critical chemical potentials for σ and Δ, $\mu_{c\sigma}$ and $\mu_{c\Delta}$, are different. This is different from the Wilson fermion, where $\mu_{c\sigma}$ and $\mu_{c\Delta}$ are almost the same.

Note that, for both the Dirac and naive fermions, the phase transition of σ at finite μ without the Kondo effect is first order, where the order parameter σ discontinuously drops to zero. On the other hand, when the Kondo effect is switched on, its order is smeared.

[7] In $1+1$ dimensions, where the coupling constants are dimensionless, the μ/Λ dependences of dimensionless condensates regularized by the cutoff Λ do not depend on the value of the cutoff.

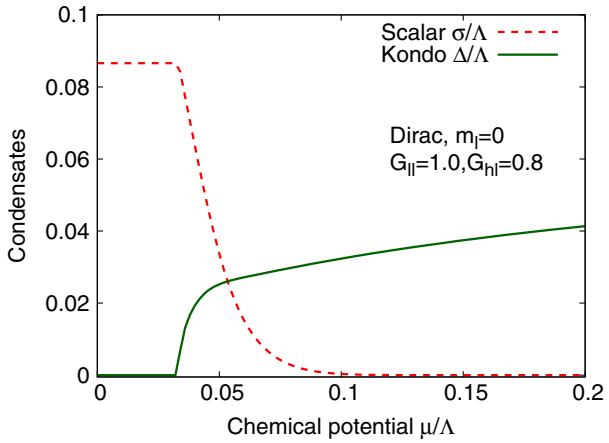

FIG. 7. μ dependences of σ and Δ for the massless Dirac fermion at a strong heavy-light coupling $G_{hl}=0.8$.

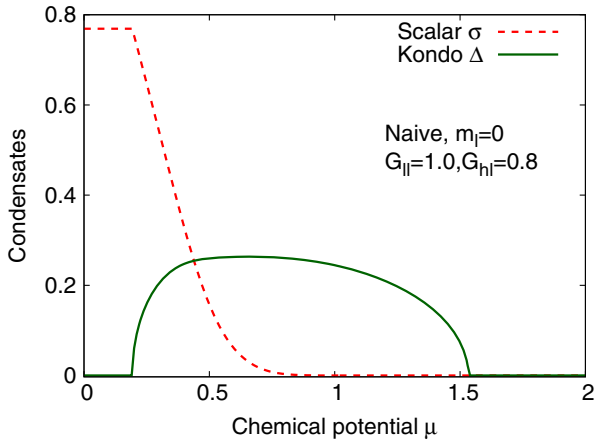

FIG. 8. μ dependences of σ and Δ for the massless naive fermions at a strong heavy-light coupling $G_{hl}=0.8$.

[1] J. Kondo, Resistance minimum in dilute magnetic alloys, Prog. Theor. Phys. **32**, 37 (1964).

[2] A. C. Hewson, *The Kondo Problem to Heavy Fermions* (Cambridge University Press, Cambridge, England, 1993).

[3] K. Yosida, *Theory of Magnetism* (Springer-Verlag, Berlin, 1996).

[4] K. Yamada, *Electron Correlation in Metals* (Cambridge University Press, Cambridge, England, 2004).

[5] Piers Coleman, *Introduction to Many-Body Physics* (Cambridge University Press, Cambridge, England, 2015).

[6] Lars Fritz and Matthias Vojta, The physics of Kondo impurities in graphene, Rep. Prog. Phys. **76**, 032501 (2013).

[7] A. Principi, G. Vignale, and E. Rossi, Kondo effect and non-Fermi-liquid behavior in Dirac and Weyl semimetals, Phys. Rev. B **92**, 041107(R) (2015).

[8] T. Yanagisawa, Dirac fermions and Kondo effect, J. Phys. Conf. Ser. **603**, 012014 (2015).

[9] T. Yanagisawa, Kondo effect in dirac systems, J. Phys. Soc. Jpn. **84**, 074705 (2015).

[10] Andrew K. Mitchell and Lars Fritz, Kondo effect in three-dimensional Dirac and Weyl systems, Phys. Rev. B **92**, 121109(R) (2015).

[11] Jin-Hua Sun, Dong-Hui Xu, Fu-Chun Zhang, and Yi Zhou, A magnetic impurity in a Weyl semimetal, Phys. Rev. B **92**, 195124 (2015).

[12] Xiao-Yong Feng, Hanting Zhong, Jianhui Dai, and Qimiao Si, Dirac-Kondo semimetals and topological Kondo insulators in the dilute carrier limit, arXiv:1605.02380.
[13] Takuya Kanazawa and Shun Uchino, Overscreened Kondo effect, (color) superconductivity, and Shiba states in Dirac metals and quark matter, Phys. Rev. D **94**, 114005 (2016).
[14] Hsin-Hua Lai, Sarah E. Grefe, Silke Paschen, and Qimiao Si, Weyl-Kondo semimetal in heavy-fermion systems, Proc. Natl. Acad. Sci. U.S.A. **115**, 93 (2018).
[15] Seulgi Ok, Markus Legner, Titus Neupert, and Ashley M. Cook, Magnetic Weyl and Dirac Kondo semimetal phases in heterostructures, arXiv:1703.03804.
[16] Da Ma, Hua Chen, Haiwen Liu, and X. C. Xie, Kondo effect with Weyl semimetal Fermi arcs, Phys. Rev. B **97**, 045148 (2018).
[17] Lin Li, Jin-Hua Sun, Zhen-Hua Wang, Dong-Hui Xu, Hong-Gang Luo, and Wei-Qiang Chen, Magnetic states and Kondo screening in Weyl semimetals with chiral anomaly, Phys. Rev. B **98**, 075110 (2018).
[18] S. Dzsaber, X. Yan, M. Taupin, G. Eguchi, A. Prokofiev, T. Shiroka, P. Blaha, O. Rubel, S. E. Grefe, H.-H. Lai, Q. Si, and S. Paschen, Giant spontaneous Hall effect in a nonmagnetic Weyl–Kondo semimetal, Proc. Natl. Acad. Sci. U. S. A. **118**, e2013386118 (2021).
[19] Hai-Feng Lü, Ying-Hua Deng, Sha-Sha Ke, Yong Guo, and Huai-Wu Zhang, Quantum impurity in topological multi-Weyl semimetals, Phys. Rev. B **99**, 115109 (2019).
[20] Ki-Seok Kim and Jae-Ho Han, Interplay between chiral magnetic and Kondo effects in Weyl metal phase, Curr. Appl. Phys. **19**, 236 (2019).
[21] Sarah E. Grefe, Hsin-Hua Lai, Silke Paschen, and Qimiao Si, Weyl-Kondo semimetals in nonsymmorphic systems, Phys. Rev. B **101**, 075138 (2020).
[22] Sarah E. Grefe, Hsin-Hua Lai, Silke Paschen, and Qimiao Si, Extreme topological tunability of Weyl-Kondo semimetal to Zeeman coupling, arXiv:2012.15841.
[23] G. T. D. Pedrosa, Joelson F. Silva, and E. Vernek, Kondo screening regimes in multi-Dirac and Weyl systems, Phys. Rev. B **103**, 045137 (2021).
[24] S. Yasui and K. Sudoh, Heavy-quark dynamics for charm and bottom flavor on the Fermi surface at zero temperature, Phys. Rev. C **88**, 015201 (2013).
[25] Shigehiro Yasui, Kondo effect in charm and bottom nuclei, Phys. Rev. C **93**, 065204 (2016).
[26] Shigehiro Yasui and Kazutaka Sudoh, Kondo effect of $\bar{D}_s$ and $\bar{D}_s^*$ mesons in nuclear matter, Phys. Rev. C **95**, 035204 (2017).
[27] Shigehiro Yasui and Tomokazu Miyamoto, Spin-isospin Kondo effects for Σ_c and Σ_c^* baryons and $\bar{D}$ and $\bar{D}^*$ mesons, Phys. Rev. C **100**, 045201 (2019).
[28] Koichi Hattori, Kazunori Itakura, Sho Ozaki, and Shigehiro Yasui, QCD Kondo effect: Quark matter with heavy-flavor impurities, Phys. Rev. D **92**, 065003 (2015).
[29] Sho Ozaki, Kazunori Itakura, and Yoshio Kuramoto, Magnetically induced QCD Kondo effect, Phys. Rev. D **94**, 074013 (2016).
[30] Shigehiro Yasui, Kei Suzuki, and Kazunori Itakura, Kondo phase diagram of quark matter, Nucl. Phys. **A983**, 90 (2019).
[31] Shigehiro Yasui, Kondo cloud of single heavy quark in cold and dense matter, Phys. Lett. B **773**, 428 (2017).
[32] Taro Kimura and Sho Ozaki, Fermi/non-Fermi mixing in SU(N) Kondo effect, J. Phys. Soc. Jpn. **86**, 084703 (2017).
[33] Shigehiro Yasui, Kei Suzuki, and Kazunori Itakura, Topology and stability of the Kondo phase in quark matter, Phys. Rev. D **96**, 014016 (2017).
[34] Kei Suzuki, Shigehiro Yasui, and Kazunori Itakura, Interplay between chiral symmetry breaking and the QCD Kondo effect, Phys. Rev. D **96**, 114007 (2017).
[35] Shigehiro Yasui and Sho Ozaki, Transport coefficients from the QCD Kondo effect, Phys. Rev. D **96**, 114027 (2017).
[36] Taro Kimura and Sho Ozaki, Conformal field theory analysis of the QCD Kondo effect, Phys. Rev. D **99**, 014040 (2019).
[37] R. Fariello, Juan C. Macxías, and F. S. Navarra, The QCD Kondo phase in quark stars, arXiv:1901.01623.
[38] Koichi Hattori, Xu-Guang Huang, and Robert D. Pisarski, Emergent QCD Kondo effect in two-flavor color superconducting phase, Phys. Rev. D **99**, 094044 (2019).
[39] Daiki Suenaga, Kei Suzuki, and Shigehiro Yasui, QCD Kondo excitons, Phys. Rev. Research **2**, 023066 (2020).
[40] Daiki Suenaga, Kei Suzuki, Yasufumi Araki, and Shigehiro Yasui, Kondo effect driven by chirality imbalance, Phys. Rev. Research **2**, 023312 (2020).
[41] Takuya Kanazawa, Random matrix model for the QCD Kondo effect, arXiv:2006.00200.
[42] Yasufumi Araki, Daiki Suenaga, Kei Suzuki, and Shigehiro Yasui, Two relativistic Kondo effects: Classification with particle and antiparticle impurities, Phys. Rev. Research **3**, 013233 (2021).
[43] Yasufumi Araki, Daiki Suenaga, Kei Suzuki, and Shigehiro Yasui, Spin-orbital magnetic response of relativistic fermions with band hybridization, Phys. Rev. Research **3**, 023098 (2021).
[44] Daiki Suenaga, Yasufumi Araki, Kei Suzuki, and Shigehiro Yasui, Chiral separation effect catalyzed by heavy impurities, Phys. Rev. D **103**, 054041 (2021).
[45] Kenneth G. Wilson, *Gauge Theories and Modern Field Theory* (MIT Press, Cambridge, 1975).
[46] Kenneth G. Wilson, *New Phenomena in Subnuclear Physics, Part A* (Plenum Press, New York, 1977), p. 69.
[47] Sinya Aoki, New phase structure for lattice QCD with Wilson fermions, Phys. Rev. D **30**, 2653 (1984).
[48] Sinya Aoki and Kiyoshi Higashijima, The recovery of the chiral symmetry in lattice Gross-Neveu model, Prog. Theor. Phys. **76**, 521 (1986).
[49] Sinya Aoki, U(1) problem and lattice QCD, Nucl. Phys. **B314**, 79 (1989).
[50] S. Aoki, S. Boettcher, and A. Gocksch, Spontaneous breaking of flavor symmetry and parity in the Nambu–Jona-Lasinio model with Wilson fermions, Phys. Lett. B **331**, 157 (1994).
[51] Ivan Horváth, Phase structure of the Schwinger model on the lattice with Wilson fermions in the Hartree-Fock approximation, Phys. Rev. D **53**, 3808 (1996).
[52] Taku Izubuchi, Junichi Noaki, and Akira Ukawa, Two-dimensional lattice Gross-Neveu model with Wilson fermion action at finite temperature and chemical potential, Phys. Rev. D **58**, 114507 (1998).

[53] A. Bermudez, E. Tirrito, M. Rizzi, M. Lewenstein, and S. Hands, Gross-Neveu-Wilson model and correlated symmetry-protected topological phases, Ann. Phys. (Amsterdam) **399**, 149 (2018).
[54] L. Ziegler, E. Tirrito, M. Lewenstein, S. Hands, and A. Bermudez, Correlated Chern insulators in two-dimensional Raman lattices: A cold-atom regularization of strongly-coupled four-Fermi field theories, arXiv:2011.08744.
[55] V. Azcoiti, G. Di Carlo, and A. Vaquero, QCD with two flavors of Wilson fermions: The QCD vacuum, the Aoki vacuum and other vacua, Phys. Rev. D **79**, 014509 (2009).
[56] Stephen R. Sharpe, On the consistency of the Aoki-phase, Phys. Rev. D **79**, 054503 (2009).
[57] Vicente Azcoiti, Giuseppe Di Carlo, Eduardo Follana, and Alejandro Vaquero, Elucidating the vacuum structure of the Aoki phase, Nucl. Phys. **B870**, 138 (2013).
[58] V. Azcoiti, G. Di Carlo, E. Follana, M. Giordano, and A. Vaquero, Phase structure of a generalized Nambu–Jona-Lasinio model with Wilson fermions in the mean-field or large-N expansion, Nucl. Phys. **B875**, 45 (2013).
[59] P. Vranas, I. Tziligakis, and John B. Kogut, Fermion scalar interactions with domain wall fermions, Phys. Rev. D **62**, 054507 (2000).
[60] Taku Izubuchi and Kei-ichi Nagai, Two-dimensional lattice Gross-Neveu model with domain wall fermions, Phys. Rev. D **61**, 094501 (2000).
[61] Sinya Aoki, Taku Izubuchi, Yoshinobu Kuramashi, and Yusuke Taniguchi, Domain wall fermions in quenched lattice QCD, Phys. Rev. D **62**, 094502 (2000).
[62] Michael Creutz, Taro Kimura, and Tatsuhiro Misumi, Aoki phases in the lattice Gross-Neveu model with flavored mass terms, Phys. Rev. D **83**, 094506 (2011).
[63] Tatsuhiro Misumi, Takashi Z. Nakano, Taro Kimura, and Akira Ohnishi, Strong-coupling analysis of parity phase structure in staggered-Wilson fermions, Phys. Rev. D **86**, 034501 (2012).
[64] Tatsuhiro Misumi, Phase structure for lattice fermions with flavored chemical potential terms, J. High Energy Phys. 08 (2012) 068.
[65] Syo Kamata and Hidekazu Tanaka, Non-γ_5 hermiticity fermions in two dimensions, Prog. Theor. Exp. Phys. **2013**, 123B05 (2013).
[66] Yoshihito Kuno, Phase structure of the interacting Su-Schrieffer-Heeger model and the relationship with the Gross-Neveu model on lattice, Phys. Rev. B **99**, 064105 (2019).
[67] Yasufumi Araki and Taro Kimura, Phase structure of two-dimensional topological insulators by lattice strong-coupling expansion, Phys. Rev. B **87**, 205440 (2013).
[68] Akihiko Sekine and Kentaro Nomura, Axionic antiferromagnetic insulator phase in a correlated and spin-orbit coupled system, J. Phys. Soc. Jpn. **83**, 104709 (2014).
[69] Akihiko Sekine and Kentaro Nomura, Axion electrodynamics in topological materials, J. Appl. Phys. **129**, 141101 (2021).
[70] N. Read and D. M. Newns, On the solution of the Coqblin-Schrieffer Hamiltonian by the large-N expansion technique, J. Phys. C **16**, 3273 (1983).
[71] Piers Coleman, $\frac{1}{N}$ expansion for the Kondo lattice, Phys. Rev. B **28**, 5255 (1983); **29**, 2829(E) (1984).
[72] David J. Gross and André Neveu, Dynamical symmetry breaking in asymptotically free field theories, Phys. Rev. D **10**, 3235 (1974).
[73] Tohru Eguchi and Ryuichi Nakayama, The Wilson lattice fermion and the recovery of chiral symmetry near the continuum limit, Phys. Lett. **126B**, 89 (1983).
[74] Estia Eichten and Brian Russell Hill, An effective field theory for the calculation of matrix elements involving heavy quarks, Phys. Lett. B **234**, 511 (1990).
[75] Howard Georgi, An effective field theory for heavy quarks at low energies, Phys. Lett. B **240**, 447 (1990).
[76] Matthias Neubert, Heavy-quark symmetry, Phys. Rep. **245**, 259 (1994).
[77] Aneesh V. Manohar and Mark B. Wise, *Heavy Quark Physics* (Cambridge University Press, Cambridge, England, 2000).
[78] D. Ebert, T. Feldmann, R. Friedrich, and H. Reinhardt, Effective meson Lagrangian with chiral and heavy quark symmetries from quark flavor dynamics, Nucl. Phys. **B434**, 619 (1995).
[79] Dietmar Ebert, Thorsten Feldmann, and Hugo Reinhardt, Extended NJL model for light and heavy mesons without $q-\bar{q}$ thresholds, Phys. Lett. B **388**, 154 (1996).
[80] A. L. Mota and E. Ruiz Arriola, Relativistic NJL model with light and heavy quarks, Eur. Phys. J. A **31**, 711 (2007).
[81] Xiao-Yu Guo, Xiao-Lin Chen, and Wei-Zhen Deng, Heavy mesons in the Nambu–Jona-Lasinio model, Chin. Phys. C **37**, 033102 (2013).
[82] B. Coqblin and J. R. Schrieffer, Exchange interaction in alloys with cerium impurities, Phys. Rev. **185**, 847 (1969).
[83] J. Jünemann, A. Piga, S. J. Ran, M. Lewenstein, M. Rizzi, and A. Bermudez, Exploring Interacting Topological Insulators with Ultracold Atoms: The Synthetic Creutz-Hubbard Model, Phys. Rev. X **7**, 031057 (2017).
[84] Tsutomu Ishikawa, Katsumasa Nakayama, and Kei Suzuki, Lattice-fermionic Casimir effect and topological insulators, Phys. Rev. Research **3**, 023201 (2021).
[85] Su-Yang Xu, Y. Xia, L. A. Wray, D. Qian, S. Jia, J. H. Dil, F. Meier, J. Osterwalder, B. Slomski, H. Lin, R. J. Cava, and M. Z. Hasan, Topological phase transition and texture inversion in a tunable topological insulator, Science **332**, 560 (2011).
[86] P. Nozières and A. Blandin, Kondo effect in real metals, J. Phys. (France) **41**, 193 (1980).
[87] Shinji Takeda and Yusuke Yoshimura, Grassmann tensor renormalization group for the one-flavor lattice Gross-Neveu model with finite chemical potential, Prog. Theor. Exp. Phys. **2015**, 043B01 (2015).
[88] A. Bermudez, L. Mazza, M. Rizzi, N. Goldman, M. Lewenstein, and M. A. Martin-Delgado, Wilson Fermions and Axion Electrodynamics in Optical Lattices, Phys. Rev. Lett. **105**, 190404 (2010).
[89] Leonardo Mazza, Alejandro Bermudez, Nathan Goldman, Matteo Rizzi, Miguel Angel Martin-Delgado, and Maciej Lewenstein, An optical-lattice-based quantum simulator for relativistic field theories and topological insulators, New J. Phys. **14**, 015007 (2012).
[90] Yoshihito Kuno, Ikuo Ichinose, and Yoshiro Takahashi, Generalized lattice Wilson-Dirac fermions in $(1+1)$

dimensions for atomic quantum simulation and topological phases, Sci. Rep. **8**, 10699 (2018).
[91] T. V. Zache, F. Hebenstreit, F. Jendrzejewski, M. K. Oberthaler, J. Berges, and P. Hauke, Quantum simulation of lattice gauge theories using Wilson fermions, Quantum Sci. Technol. **3**, 034010 (2018).
[92] B. Paredes, C. Tejedor, and J. I. Cirac, Fermionic atoms in optical superlattices, Phys. Rev. A **71**, 063608 (2005).
[93] L.-M Duan, Controlling ultracold atoms in multi-band optical lattices for simulation of Kondo physics, Euro. Phys. Lett. **67**, 721 (2004).
[94] A. V. Gorshkov, M. Hermele, V. Gurarie, C. Xu, P. S. Julienne, J. Ye, P. Zoller, E. Demler, M. D. Lukin, and A. M. Rey, Two-orbital SU(N) magnetism with ultracold alkaline-earth atoms, Nat. Phys. **6**, 289 (2010).
[95] Michael Foss-Feig, Michael Hermele, and Ana Maria Rey, Probing the Kondo lattice model with alkaline-earth-metal atoms, Phys. Rev. A **81**, 051603(R) (2010).
[96] Michael Foss-Feig, Michael Hermele, Victor Gurarie, and Ana Maria Rey, Heavy fermions in an optical lattice, Phys. Rev. A **82**, 053624 (2010).
[97] Johannes Bauer, Christophe Salomon, and Eugene Demler, Realizing a Kondo-Correlated State with Ultracold Atoms, Phys. Rev. Lett. **111**, 215304 (2013).
[98] Yusuke Nishida, SU(3) Orbital Kondo Effect with Ultracold Atoms, Phys. Rev. Lett. **111**, 135301 (2013).
[99] Masaya Nakagawa and Norio Kawakami, Laser-Induced Kondo Effect in Ultracold Alkaline-Earth Fermions, Phys. Rev. Lett. **115**, 165303 (2015).
[100] Masaya Nakagawa, Norio Kawakami, and Masahito Ueda, Non-Hermitian Kondo Effect in Ultracold Alkaline-Earth Atoms, Phys. Rev. Lett. **121**, 203001 (2018).